Plant, Cell and Environment (2004) **27**, 279–292

Properties of ion channels in the protoplasts of the Mediterranean seagrass *Posidonia oceanica*

A. CARPANETO[1], A. NASO[1], A. PAGANETTO[1], L. CORNARA[2], E.-R. PESCE[1,*] & F. GAMBALE[1]

[1]*Istituto di Biofisica C.N.R., Via De Marini 6, 16149 Genova, Italy and* [2]*DIPTERIS, sede di Botanica, Università di Genova, corso Dogali 1 M, 16136 Genova, Italy*

ABSTRACT

***Posidonia oceanica* (L) Delile, a seagrass endemic of the Mediterranean sea, provides food and shelter to marine organisms. As environment contamination and variation in physico-chemical parameters may compromise the survival of the few *Posidonia* genotypes living in the Mediterranean, comprehending the molecular mechanisms controlling *Posidonia* growth and development is increasingly important. In the present study the properties of ion channels in *P. oceanica* plasma membranes studied by the patch-clamp technique in protoplasts obtained from the young non-photosynthetic leaves were investigated. In protoplasts that were presumably originated from sheath cells surrounding the vascular bundles of the leaves, an outward-rectifying time-dependent channel with a single channel conductance of 58 ± 2 pS which did not inactivate, was selective for potassium and impermeable to monovalent cations such as Na^+, Li^+ and Cs^+ was identified. In the same protoplasts, an inward-rectifying channel that has a time-dependent component with single channel conductance of the order of 10 pS, a marked selectivity for potassium and no permeation to sodium was also identified, as was a third type of channel that did not display any ionic selectivity and was reversibly inhibited by tetraethylammonium and lanthanum. A comparison of *Posidonia* channel characteristics with channels identified in terrestrial plants and other halophytic plants is included.**

Key-words: *Posidonia oceanica*; ion channels; patch-clamp; seagrasses.

INTRODUCTION

Posidonia oceanica (L) Delile, a seagrass endemic of the Mediterranean Sea, forms large marine meadows and participates in hydrodynamic stabilization of the coasts. *Posidonia oceanica* is essential for coastal preservation as it stabilizes mud by damping the waves and their subsequent erosive action. *Posidonia* meadows are responsible for the majority of organic matter and oxygen production in the Mediterranean Sea, and represent an ideal habitat for several marine organisms.

Posidonia oceanica propagation proceeds mainly by asexual clonal growth while sexual reproduction is sporadic and occurs primarily through self-pollination within the same floral axis or between fragmented clonal patches (Procaccini & Mazzella 1996, 1998). Clonal propagation determines a particularly low level of genetic variability in *P. oceanica* as compared with other Mediterranean seagrasses (Procaccini & Mazzella 1996). Consequently, as *Posidonia* is well adapted to a stable marine environment, significant environmental changes may determine a dramatic reduction and even extinction of the few existing *Posidonia* clonal species.

Seagrasses are higher aquatic plants that returned to the sea after their predecessors spent a period of time on land. The various morphological adaptations of these halophytes to diverse marine environments have been thoroughly documented. Adaptations of marine plants are possibly determined by changes in genes expressing proteins that support plant acclimatization to stressful parameters (such as high salinity and high hydrostatic pressure) that are noxious to terrestrial plants. Although it is not surprising that membrane transport-mechanisms in marine plants show similarities with those of homologous transport proteins already identified in terrestrial plants, it is to be expected that certain transport proteins might have changed during evolution in order to support the growth of seagrasses in the sea.

The negative effects of salinity in non-halophytic plants essentially concern high osmotic pressure and the toxicity of Na^+ and Cl^-. There is evidence that Na^+ may enter root plant cells owing to a high (negative) membrane potential which is able to support a Na^+ cytoplasmic concentration that is a hundred-fold greater than the external solution. Indeed, a variety of channels partially permeable to sodium are present at plant root level and in other tissues. These may include voltage-insensitive, monovalent, cation-permeable channels (VIC), as well as inward-rectifying K^+ channels (KIR) or outward-rectifying K^+ channels (KOR) (Amtmann & Sanders 1999; White 1999; Blumwald, Aharon & Apse 2000), as the selectivity of some channels, that are generally thought to be responsible for K^+ uptake into the cell, may change depending on tissue and plant species.

Na^+ accumulation in the cytoplasm of seagrasses may be

Correspondence: F. Gambale. Fax: + 39 0106475500; e-mail: gambale@area.ge.cnr.it

**Present address, Institute of Plant Sciences, University of Bern, Altenbergrain 21, CH-3013 Bern, Switzerland.*

partially prevented by high selectivity of ion channels or by an active outflow of cytosolic Na^+ either out of the cell or to the vacuole. For example, it has been shown that salt treatments increase the activity of Na^+/H^+-antiporters in several plants (Buchanan, Gruissem & Jones 2000), which in turn clearly depends on the energy provided by the plasma membrane and vacuolar H^+-ATPases.

Previous observations strongly suggest investigating transport mechanisms in seagrasses in order to gain a better understanding of some basic properties (e.g. ion selectivity) in passive and active membrane transporters.

Unfortunately, only a few studies have attempted to contribute to the molecular characterization of membrane channels in seawater halophytes (Garrill, Tyerman & Findlay 1994; Carpaneto, Cantù & Gambale 1999). In previous studies of the mechanisms involved in the adaptation of *P. oceanica* to the marine environment, we have characterized some ion channels in vacuoles from *P. oceanica* non-photosynthetic leaves (Carpaneto *et al*. 1997, 1999); here we investigate ion channels in the protoplasts obtained from *Posidonia* leaves in order to verify their properties in comparison with similar channels identified in terrestrial plants and other halophytic angiosperms (such as Zosteraceae) whose leaf channels were characterized by means of the patch-clamp technique (Garrill *et al*. 1994).

MATERIALS AND METHODS

Plant material

Posidonia oceanica was collected from meadows located near Camogli Genoa, Italy, at a depth ranging from 10 to 20 m. The plant was maintained in oxygenated natural seawater at a constant temperature of 15 °C and used within 2 months of collection.

Morphological characterization and microscopic study

The basal parts of the youngest non-photosynthetic leaves were cut into pieces of approximately 1 cm^2 and used for both protoplast isolation and anatomical observations. For light microscopy the pieces were fixed in FAA (5 mL formalin, 5 mL acetic acid, 90 mL 60% ethanol) for 24 h, dehydrated in a graded ethanol series and embedded in JB4 resin (Polysciences Inc., Warrington, PA, USA) in BEEM capsules (Better Equipment For Electron Microscopy Sciences, Fort Washington, PA, USA) (Brinn & Pickett 1979). Sections of 10–20 μm were cut with a Reichert Om U_2 ultramicrotome (Reichert, Wien, Austria) equipped with a glass knife. Toluidine Blue O (TBO) at pH 4.4 was used as the metachromatic stain (Feder & O'Brien 1968).

Micrographs were recorded using a DM RB Leitz microscope (Leitz, Wetzlar, Germany) equipped with a Dage MTI camera and analogue-digital converter (DAGE-MTI Inc., Michigan City, IN, USA). Images were digitized using the National Institute of Health IMAGE software driving a SCION PCI video acquisition board (Scion Corp., Frederick, MD, Usa). Cell measurements were carried out by digital imaging on both cross and longitudinal sections, obtaining mean cell volumes for different cell layers in the leaf. Data were analysed using the Instat 3.05 and the Prism 3.02 packages (GraphPad Software Inc., San Diego, CA, USA).

For scanning electron microscopy (SEM), after ethanol dehydration specimens were critical-point dried with liquid CO_2 using a CPD750 Emscope (Bio-Rad, Hercules, CA, USA), mounted on stubs, coated with gold by AGAR PS3 sputtering (15–20 nm), and viewed with a Philips 515 SEM (Philips, Eindhoven, The Netherlands) at an acceleration voltage of 20 kV. Photographs were taken using Kodak Technical PAN film (Eastman Kodak Co., Rochester, NY, USA).

Protoplast isolation and identification

The procedure for protoplast isolation was modified from that previously described by other authors (Balestri & Cinelli 2001; Arai *et al*. 1991). Essentially, the basal part of the youngest non-photosynthetic *P. oceanica* leaves was cut into small pieces (1 cm^2 or less) in artificial sea water (ASW: 450 mM NaCl, 10 mM KCl, 50 mM $MgCl_2$, 10 mM $CaCl_2$, 20 mM Trizma, pH = 7.9). Leaf fragments were incubated at 30 °C for 4 h (or, alternatively, overnight at room temperature) in a solution containing: 2% (w/v) cellulase Onozuka RS (Yakult, Honsha, Tokyo, Japan), 0.5% Macerozyme R-10 (Yakult, Honsha), 800 mM sorbitol, 50 mM NaAcetate, 50 mM ascorbic acid, 40 mM NaOH, pH = 5.5. The digest was filtered through a 120-μm nylon mesh and centrifuged twice in standard external solution (SE) or ASW (10 min at 300 *g* and 10 °C). The protoplast suspension was stored in ice for a maximum of 12 h and aliquots used for patch-clamp measurements.

Patch-clamp recordings

Patch-clamp recordings were performed on isolated protoplasts in the whole-cell configurations. Applied voltages and currents were controlled and recorded with a List EPC7 patch-clamp amplifier (List-electronic, Darmstadt/Eberstadt, Germany) interfaced with an Instrutech AD/DA board (Instrutech, Elmont, NY, USA). A Macintosh personal computer running the PULSE software (Heka Electronic, Lambrecht, Germany) was used to generate the stimulation protocol and to store the digitized current records on the hard disk. Data were low-pass filtered with a four-pole Bessel filter set at frequencies between 0.1 and 3 kHz and sampled at a frequency from two to five times that of the low-pass filter for final storage. The command voltages were corrected off-line for liquid junction potential. Data analysis was performed using home-produced programs written in IgorPro (Wavemetrics Inc., Lake Oswego, OR, USA). The leakage subtraction was only applied when explicitly mentioned in the text or the figure legend. The leakage of the inward currents was eliminated by subtracting in each record the initial (instantaneous) current from the final steady-state current. As the initial

outward current is more difficult to identify, the linear part of the I–V characteristic (where outward currents are not activated yet) was subtracted from the complete outward current-voltage characteristics.

Patch pipettes were pulled from borosilicate glass and slightly fire-polished before use. The resistance of the pipettes in standard solutions was between 4 and 8 MOhm. The standard pipette solution contained: 150 mM KCl, 5 mM $MgCl_2$, 10 μM $CaCl_2$, 1 mM EGTA, 780 mM sorbitol, 20 mM Trizma, 5 mM Mg-ATP, pH = 7.2. The standard bath solution contained: 450 mM KCl, 50 mM $MgCl_2$, 10 mM $CaCl_2$, 20 mM sorbitol, 20 mM Trizma, pH = 7.5.

The figures show current records selected among the 55 successful patch-clamp experiments performed; 10 displayed outward currents, 35 displayed inward currents and 10 displayed both inward and outward currents.

RESULTS

Protoplast and cell sizes

Posidonia leaves show an open sheathing base, a narrow ligule marking the junction of the sheath and leaf blade, and a distal strap-shaped blade. The inner youngest leaf in the shoot is short and generally appears whitish, due to the presence of non-photosynthetic proplastids (Mariani Colombo, Rascio & Cinelli 1983). About half of the length of the basal portion of the youngest leaf, proximal to the meristem, is enclosed by the sheaths of the oldest leaves. This creates a micro-environment that is related to the development of a standing osmotic gradient within this zone (Tyerman 1989).

Figure 1a displays a schematic representation of *Posidonia oceanica* short shoots and leaves, which are also

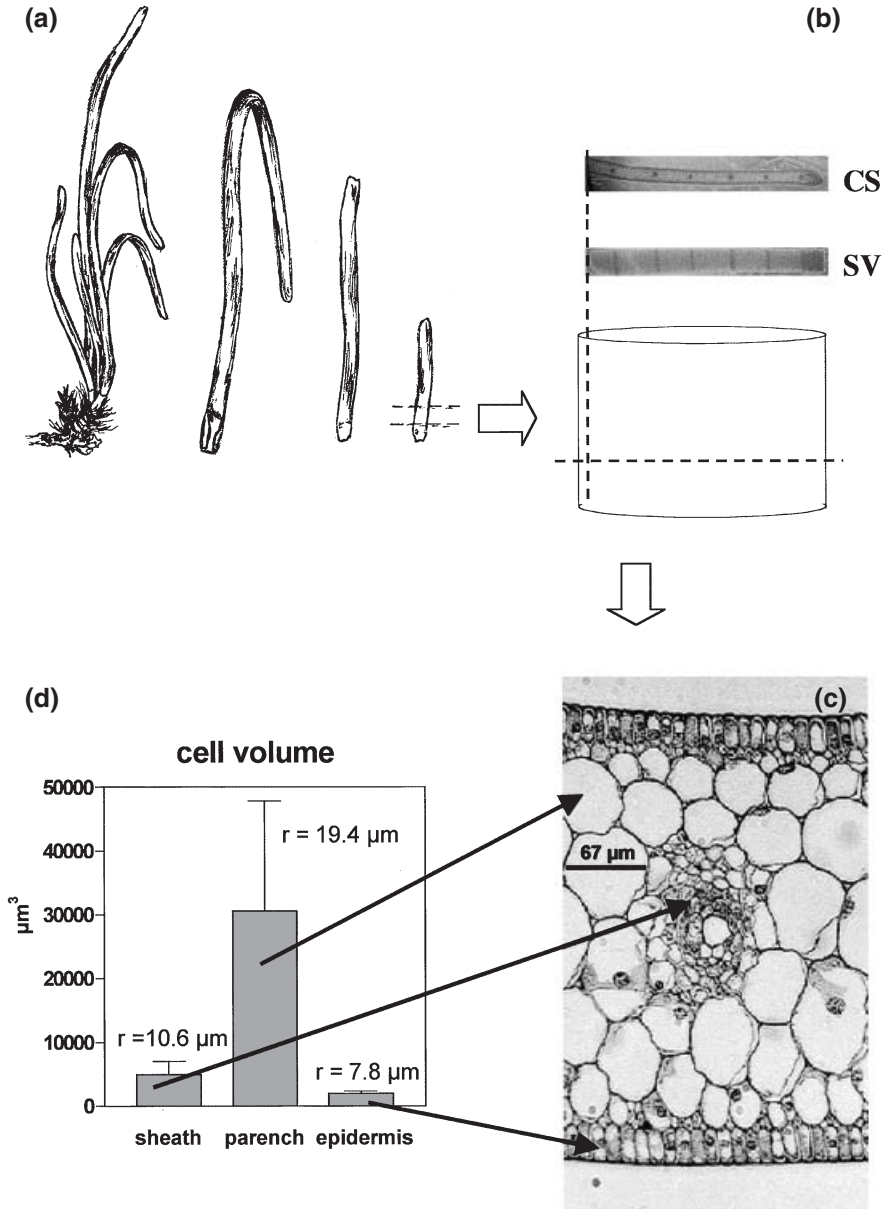

Figure 1. *Posidonia oceanica* leaves and cell size. (a) Single tuft and leaves of *Posidonia oceanica*. The basal portion of the inner youngest leaf used in this study is indicated. (b) Schematic representation of leaf sectioning for histological observations; the two upper panels show the cross-section (CS) and the surface view (SV) of a leaf fragment. (c) Micrograph of a leaf cross-section showing the monolayered epidermis and the mesophyll with large parenchymatous cells and a vascular bundle surrounded by the sheath cells. (d) Graphic representation of the cell volumes of different cell types; the mean value of the radius of each cell type is shown.

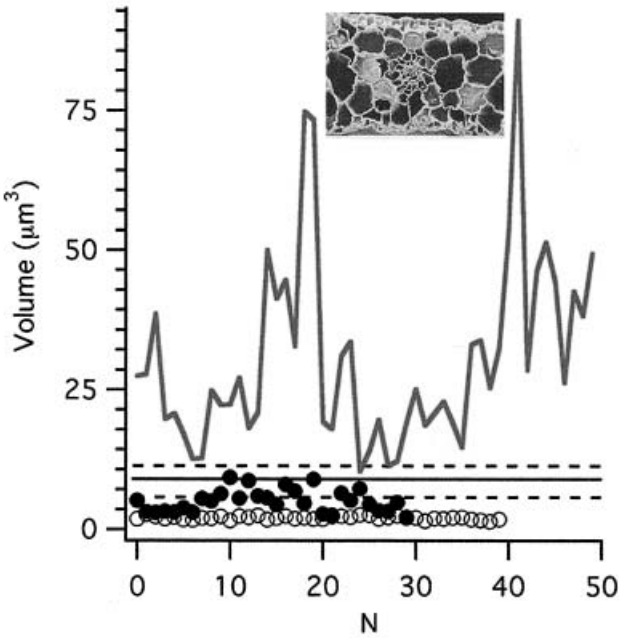

Figure 2. Size of *Posidonia oceanica* cells and protoplasts. The volume of the three cell types (sheath: filled circles, parenchyma: grey line and epidermis cells: empty circles) are compared with the volume derived from the mean radius (continuous straight line) of the patched protoplasts ± SE (dashed lines). N is a progressive number identifying each cell or protoplast. Inset: scanning electron microscopy micrograph showing the large size of parenchyma cells.

shown separately to highlight the different stages of development depending on leaf age; on the right the youngest internal whitish leaf is represented. Figure 1b shows a schematic representation of a *Posidonia* leaf section together with pictures of the cross-section (CS) and surface view (SV) of the fragments used in the enzymatic digestion. The dark lines in the surface view and the dark spots in the cross-section correspond to the vascular bundles or veins present in each leaf (up to 16 per leaf). In addition, as in all monocotyledon leaves, a number of cross veins interconnecting the parallel vein system are also present (not shown). Figure 1c shows a cross-section of the white non-photosynthetic part of the young internal leaf at a much higher magnification; parenchimatic cells, one vascular bundle, surrounded by sheath cells, and epidermal cells can be recognized. Sheath cells undergo lignification in the photosynthetic green leaves. Finally, Fig. 1d shows a graphic representation of the volume (mean ± SD) of the three cell types.

The high standard deviation of the volumes of parenchymatic cells may depend on the presence of different cell populations in the parenchyma (Balestri & Cinelli 1992). However, both the diagram (Fig. 1d) and visual inspection of the leaf section clearly indicate that the parenchymatic cell population is characterized by a significantly larger volume than that of the other two cell types. Figure 2 illustrates the mean size of the protoplasts used in the patch-clamp experiments (continuous straight line) compared with the sizes of the different cells obtained from pictures like those shown in Fig. 1c and in the inset of Fig. 2.

Figure 3a shows a family of typical outward currents recorded in selected *Posidonia* protoplasts with a mean radius of 13.0 ± 1.1 μm (mean ± SE, n = 16). These protoplasts presumably correspond (see Fig. 1d) to sheath cells surrounding the vascular bundles which have a mean equivalent radius of 10.6 ± 1.4 μm, whereas the other two cell types should produce protoplasts with significantly different sizes to those used in this work. The equivalent radius of parenchyma and epidermis cells, evaluated from microphotographs such as those shown in Figs 1c and 2 are 7.8 ± 0.7 μm (mean ± SE, n = 40) and 19.4 ± 2.3 μm (mean ± SE, n = 50), respectively.

Functional characterization of positive currents

The family of ionic currents shown in Fig. 3a were elicited by a series of voltage steps followed by slow tail currents with decay times of the order of several hundred milliseconds (see also Fig. 4c). Figure 3b illustrates the current-voltage (I–V) characteristics obtained by plotting the steady-state level of the currents (shown in Fig. 3a) as a function of the applied membrane potential (empty circles). Filled circles represent the same I–V characteristic corrected for current leakage (represented by the continuous straight line) derived from the best fit of the linear part of the curve between approximately –20 and –130 mV. The excellent correspondence between $V_{(\mathrm{Nernst})}(K^+)$ [upward arrow in (b)] and the experimental reversal potential suggests that these currents might be mediated by an outward efflux of potassium ions through a potassium-selective channel. The Boltzmann distribution illustrated in Fig. 3c shows the membrane conductance, obtained by dividing the steady state of the current by the membrane potential ($V - V_{\mathrm{Rev}}$) and by normalizing the currents to the maximum value measured in these working conditions. The distribution demonstrates that the outward currents were activated by step voltages more positive than –25 mV and saturated at voltages larger than +25 mV; between these two voltages (± 25 mV) the I–V curve reveals that in our standard ionic solutions the channel possibly allows the influx of potassium ions or other cations from the bath solution to the cytoplasm.

The potassium selectivity properties of the channel are also confirmed by tail potential experiments shown in Fig. 4a, which displays the tail currents elicited by a series of tail potentials (from –60 to +80 mV) after a prepulse potential to +60 mV. The instantaneous tail currents, plotted as a function of the tail potential (Fig. 4b), provide further evidence that the channel is selective for cations (in this case potassium), as also in this case the extrapolated reversal potential is very close to the Nernst potential for K^+ (= +25 mV). Figure 4c and d illustrate typical de-activation time constants (Fig. 4c) and half-activation times (Fig. 4d) of the outward currents plotted as a function of tail and activation step potentials, respectively. Note that in Fig. 4a the positive currents do not display any inactivation; inactivation was absent even when the currents were elicited by prolonged depolarizing pulses lasting up to 60 s (not shown).

The characteristics of the channel depend on the external

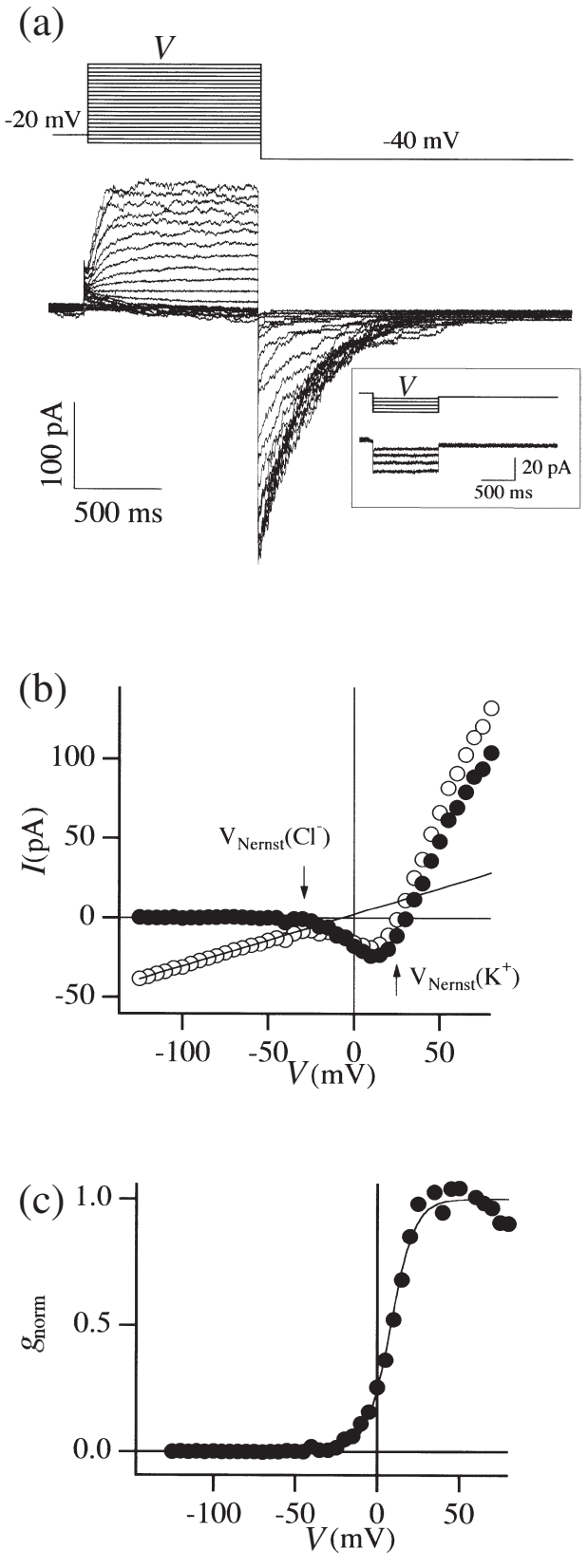

Figure 3. Macroscopic outward currents in protoplasts from *Posidonia oceanica* leaves. (a) Currents were elicited by a series of voltage steps ranging from –40 to +80 mV in 10 mV increments. Holding and tail membrane potentials: –20 and –40 mV, respectively. The upper profile illustrates the applied voltage protocol. The inset shows, at a larger magnification, some current traces used for leakage subtraction. The currents are elicited by potentials ranging from –50 to –110 mV in –20 mV steps. (b) Current-voltage characteristic of data in (a). Voltage steps from –130 to +80 mV in 5 mV increments [in (a) intermediate currents are not shown for sake of clarity while the currents elicited by voltage pulses <–40 mV are shown in the inset]. The empty circles represent the steady-state value of each current record while the filled symbols represent the same current after the leak subtraction. The leak (continuous straight line) was evaluated from the linear fitting of the current at negative membrane potentials (i.e from –20 to –130 mV). Arrows indicate the reversal potential for Cl^- and K^+ (V_{Nernst} (Cl^-) = –29 mV, V_{Nernst} (K^+) = + 25 (mV) calculated by the Nernst equation. (c) Normalized macroscopic conductance of data in (b) versus applied membrane potential. The membrane conductance was obtained by dividing the steady state of the current by the membrane potential ($V - V_{Rev}$) and by normalizing the currents to the maximum value measured in these working conditions. The continuous line represents the best fitting of the experimental data with the Boltzmann equation $g_{norm} = g/g_{max} = 1/(1 + \exp(-zF(V - V_{1/2})/RT)$ (z = 3.5, $V_{1/2}$ = 8 mV). Standard ionic solutions.

potassium concentration as illustrated in Fig. 5, in which the ionic currents activated by a step potential to +60 mV at two different K^+ concentrations are illustrated. In Fig. 5a, traces 1 and 2 represent the currents observed in 450 mM K^+ and 10 mM K^+, respectively. Note that the activation kinetics does not change appreciably as demonstrated by comparing the two currents normalized at the same maximum amplitudes (inset in Fig. 5a). Decreasing the external K^+ concentration caused the reversal potentials to shift towards more negative voltages. In Fig. 5b these values were more negative than the current activation threshold and therefore the tail currents decreased dramatically and the negative currents, activated by voltages between –25 and + 25 mV in standard ionic solutions (as in Fig. 3b), vanished. Interestingly, a decrease in external potassium concentration, and the consequent increase in the driving force at the two sides of the membrane, determined an increase in ionic current (Fig. 5b) but a decrease in conductance (Fig. 5c). This is shown in Fig. 5c, where the two conductances, normalized to the maximum value measured in 450 mM K^+, are compared. This paradoxic increase in channel conductance observed when decreasing the driving force has actually been observed in several other outward potassium channels both in animals and plants (Blatt 1991; Blatt & Gradmann 1997; Wood & Korn 2000; Ivashikina *et al*. 2001).

The positive currents are mediated by a channel which is impermeable to other monovalent cations such as Na^+, Li^+ and Cs^+ as illustrated in Fig. 6. The currents measured after substituting the external K^+ with Na^+, Li^+ and Cs^+ are shown in Fig. 6a, b and c, respectively. In the presence of these three monovalent cations the tail currents were completely suppressed, as were the negative currents elicited by volt-

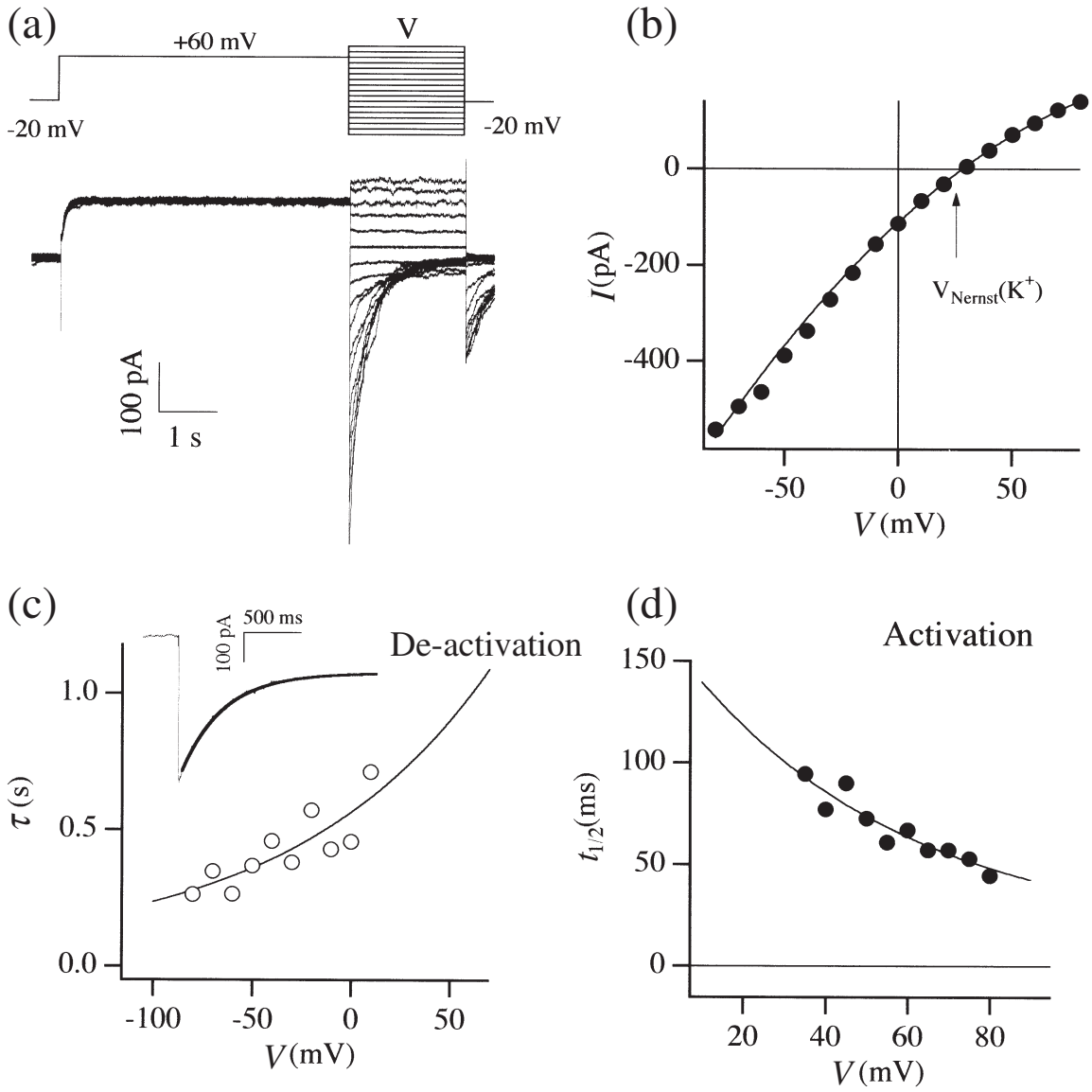

Figure 4. Selectivity and kinetics of the *Posidonia oceanica* outward-rectifying channel. (a) Tail currents elicited by membrane potentials ranging from +80 to –80 mV in 10 mV increments, after a depolarizing prepulse to +60 mV. The upper profile illustrates the applied voltage protocol. (b) Instantaneous tail current as a function of the applied membrane potential. The arrow indicates the Nernst potential for K^+ which is in excellent accordance with the experimental reversal voltage (see also Fig. 3). (c) The time course of the current de-activation was fitted with a single exponential function (inset) and the time constant, τ, plotted as a function of the applied membrane potential. Data points were fitted with the function: $\tau = \tau_0 \exp(+V/V_0)$, with $\tau_0 = 563$ ms and $V_0 = 111$ mV (continuous line). (d) The half activation time, $t_{1/2}$, was plotted as a function of the applied membrane potential. Data points could be fitted by the single exponential function [continuous line in (d)] $t = t_0 \exp(-V/V_o)$, with $t_0 = 155$ ms and $V_o = 66$ mV. Standard ionic solutions.

ages between –25 and +25 mV (see the I–V plot in each panel). Therefore, the time-dependent positive current is definitely mediated by a potassium-selective outward-rectifying channel. Furthermore, the normalized conductances were shifted to significantly more negative voltages for Na^+ and Li^+ and to a lower extent in the case of Cs^+. Moreover, it can also be observed that the activation kinetics of positive currents changed significantly in the presence of external Na^+ and Li^+: the current activated instantaneously, losing its time-dependent kinetics. On the contrary, the activation kinetics did not change when K^+ was substituted by Cs^+. The different interaction between the K^+ outward channel and Na^+ or Li^+ on one side and Cs^+ on the other, can also be observed in Fig. 6d, in which the amplitude of the tail currents is plotted as a function of the time during the perfusion (3.3 mL min^{-1}) of the K^+ bath solution with a solution containing a different monovalent cation. It can be observed that caesium abolishes the tail currents in a few seconds from the beginning of the bath perfusion; on the other hand, the substitution of K^+ with Na^+ and Li^+ takes

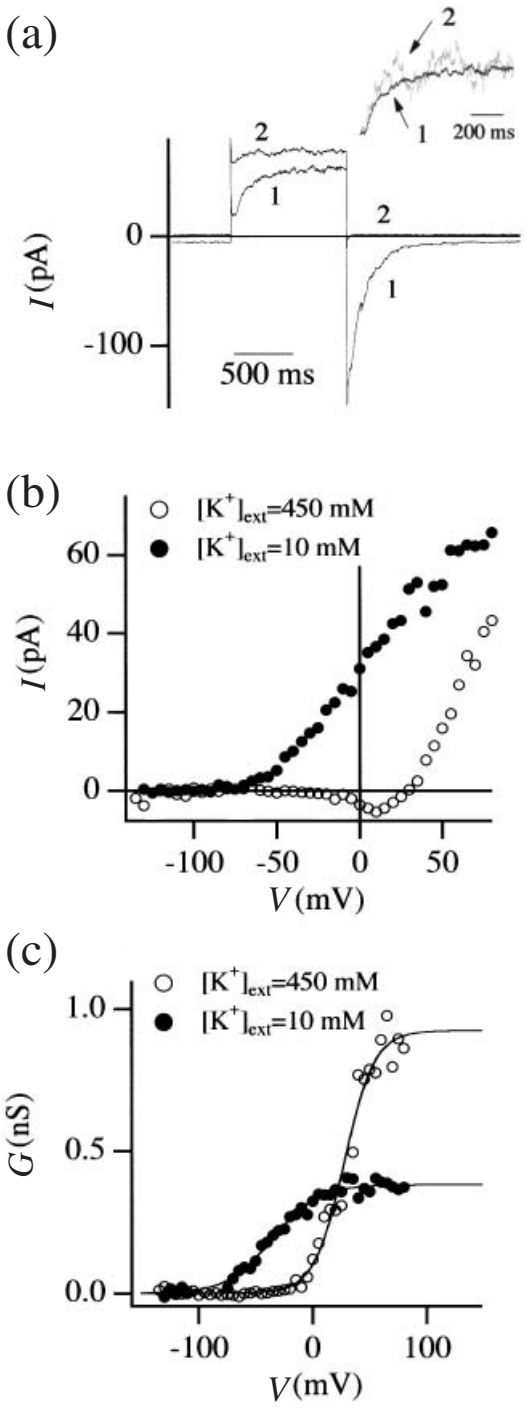

Figure 5. Sensitivity of the *Posidonia oceanica* outward-rectifying channel to the external potassium concentration. (a) Outward currents recorded in the presence of 450 mM (trace 1) and 10 mM (trace 2) external potassium. The ionic strength was kept constant by the addition of NaCl. Holding potential =–50 mV, step voltage +80 mV. Note the large tail current elicited by a voltage to –50 mV in 450 mM KCl, while no tail can be observed in 10 mM KCl. The ionic current increases when switching from 450 to 10 mM, owing to the increase in driving force. This is also shown in panel (b), where the I–V characteristics of the steady-state currents are reported as a function of the applied step voltage. (c) Normalized conductances were obtained as described in Fig. 3. Normalization was done to the maximum conductance measured in 450 mM KCl.

much longer to become effective (only data referring to Na^+ are reported for the sake of clarity). Conversely, the washout of the monovalent cation with the standard potassium solution (data not shown) required a long time for Cs^+, whereas it was very fast for Na^+ and Li^+. This suggests quite a strong interaction of caesium with the K^+ channel and a correspondingly mild interaction of Na^+ and Li^+.

The fact that the outward *Posidonia* currents were clearly due to the activation of a potassium channel was also confirmed by single channel experiments recorded in the whole cell configuration, during which the few channels that remain open at negative tail potentials (applied as step voltages or ramps) were analysed. This technical solution was adopted owing to the difficulty in excising membrane patches from protoplasts very loosely attached to the bottom of the recording chamber.

Figure 7a illustrates single outward channels (lower traces) elicited by the stimulation schematized in the upper part of the panel. A positive step voltage to +70 mV activated several single outward channels, then the membrane potential was driven to a negative potential of –40 mV, followed by a continuous voltage ramp which increased the membrane potential from –40 to +40 mV, where a few channels remained open. Records in Fig. 7a display single channel currents superimposed to the leakage current. The leak was subtracted in Fig. 7b, where the optimal correspondence between the experimental reversal potential and the Nernst potential for potassium can also be observed. Figure 7c shows a series of current records obtained at different tail potentials ranging from –45 to –25 mV. The single channel characteristic, plotted in Fig. 7b and d, gave a single channel conductance of 58 ± 2 pS. Single channel recordings also show that outward channels are clearly impermeable to Na^+ as demonstrated by tail currents where no channel openings could be recorded when external potassium was substituted by sodium (inset in Fig. 7b).

Functional characterization of negative currents

Occasionally, protoplasts from *Posidonia* leaves displayed small negative currents such as those shown in Fig. 8a. These currents comprise a time-dependent and a time-independent component. The current voltage characteristic of the time-dependent component (filled circles) obtained after the subtraction of the leakage (or time-independent component) is shown in Fig. 8b. Furthermore, in this case, tail potential protocols (Fig. 8c) demonstrated that these (time-dependent) currents are mediated by potassium-selective channels (compare $V_{Nernst}(K^+)$ and the experimental reversal potential). Accordingly, after substituting the external KCl solution with an identical concentration of NaCl, the time-dependent component was completely abolished, whereas the instantaneous time-independent component decreased by about 30% (as indicated by the two arrows in Fig. 8d); the remaining time-independent current may be ascribed to a leakage current or to a non-selective cation channel.

Single channels, representative of selective inward currents, are shown in Fig. 9. It can be observed that, in accor-

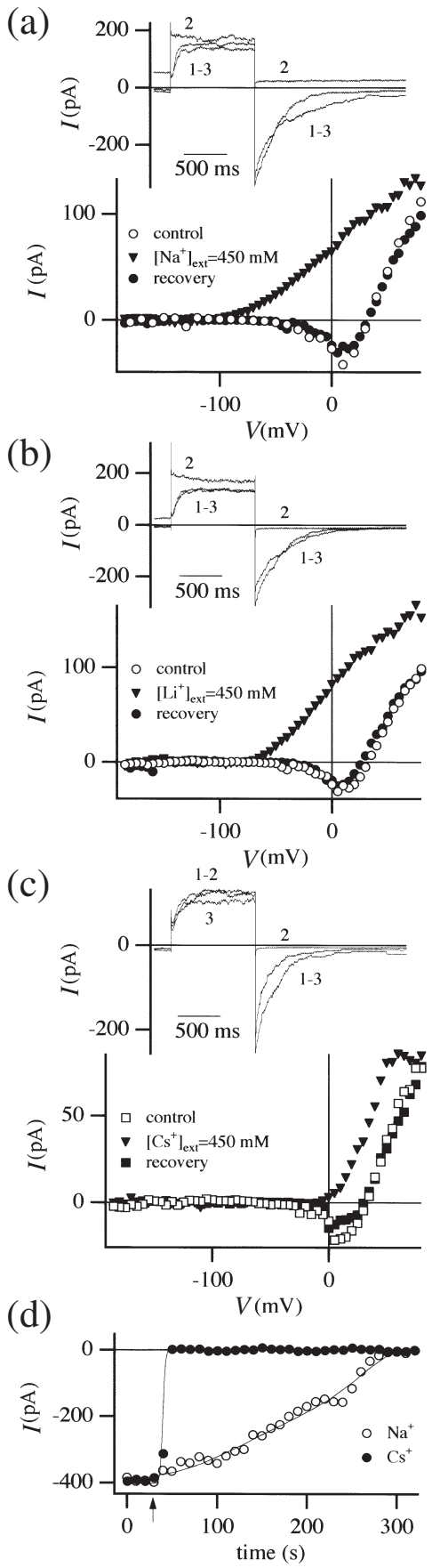

Figure 6. The outward channel of *Posidonia oceanica* leaves is impermeable to sodium, lithium and caesium. (a) Top: currents elicited by a voltage pulse to +80 mV in asymmetric standard solutions. Holding and tail voltages were –20 and –40 mV, respectively. Traces 1 and 3 were obtained in 450 mM potassium; trace 2 represents the current in 450 mM Na^+. Bottom: current-voltage characteristics in asymmetric standard solutions. Empty and filled circles represent the characteristics obtained from the steady-state value of the currents in control conditions and after the recovery ($[K^+]_{est}$ = 450 mM). Filled triangles represent the I–V characteristic obtained when K^+ in the external solution was completely replaced by Na^+ ($[Na^+]_{ext}$ = 450 mM). (b) Top: currents elicited by a voltage pulse to +80 mV in asymmetric standard solutions. Holding and tail voltages as in (a). Traces 1 and 3: 450 mM potassium; trace 2: 450 mM Li^+. Bottom: current–voltage characteristics in asymmetric standard solutions. Empty and filled circles have the same meanings as in (a). Filled triangles represent the I–V characteristic obtained when K^+ in the external solution was completely replaced by Li^+ ($[Li^+]_{ext}$ = 450 mM). (c) Top: currents recorded at +80 mV in asymmetric standard solutions. Holding and tail voltages as in (a). Traces 1 and 3: 450 mM potassium; trace 2: 450 mM Cs^+. Bottom: current–voltage characteristics in asymmetric standard solutions. Empty and filled circles have the same meanings as in (a). Filled triangles represent the I–V characteristic obtained when K^+ in the external solution was completely substituted by Cs^+ ($[Cs^+]_{ext}$ = 450 mM). (d) Instantaneous tail currents plotted as a function of time during the substitution of 450 mM KCl in the bath solution with an equimolar solution of NaCl (empty circles) and CsCl (filled circles). LiCl (not shown for clarity's sake) displayed the same behaviour as NaCl. Rate of perfusion 3.3 mL min^{-1}.

dance with the characteristics of the macroscopic inward current, the single channel opening probability increases with the amplitude of the hyperpolarizing membrane potential (Fig. 9a). The single channel conductance obtained by the linear fit of single channel amplitudes was 10 pS (data not shown). The potassium selectivity of this channel is supported by the observation that single channel transitions were impermeable to 450 mM caesium added to the external bath solution (Fig. 9b); moreover, low concentrations of external Cs^+ were sufficient to inhibit the single inward channel (not shown).

Averaging a series of 19 single channel traces recorded at a stimulation voltage of –200 mV (Fig. 9c, upper record) we were able to reconstruct (Fig. 9c, lower trace) a macroscopic current activated in a time-dependent manner with a kinetic of current activation similar to that of the corresponding (Fig. 8a) time-dependent whole-cell current. The difference in the time scale of activation of the reconstructed (approximately 100 ms) and the whole-cell (approximately 1 s) time-dependent currents might depend on the different configurations (whole-vacuole and excised-patch) adopted in the two experiments.

Finally another current was also occasionally present in *Posidonia* protoplasts. This channel has: (1) a time-dependent activation (Fig. 10a) at hyperpolarizing membrane potentials; (2) a small component which activates almost instantaneously at positive voltages (Fig. 10a & b); (3) a marked deviation from linearity at large negative potentials (Fig. 10b); (4) low selectivity, as it is permeable

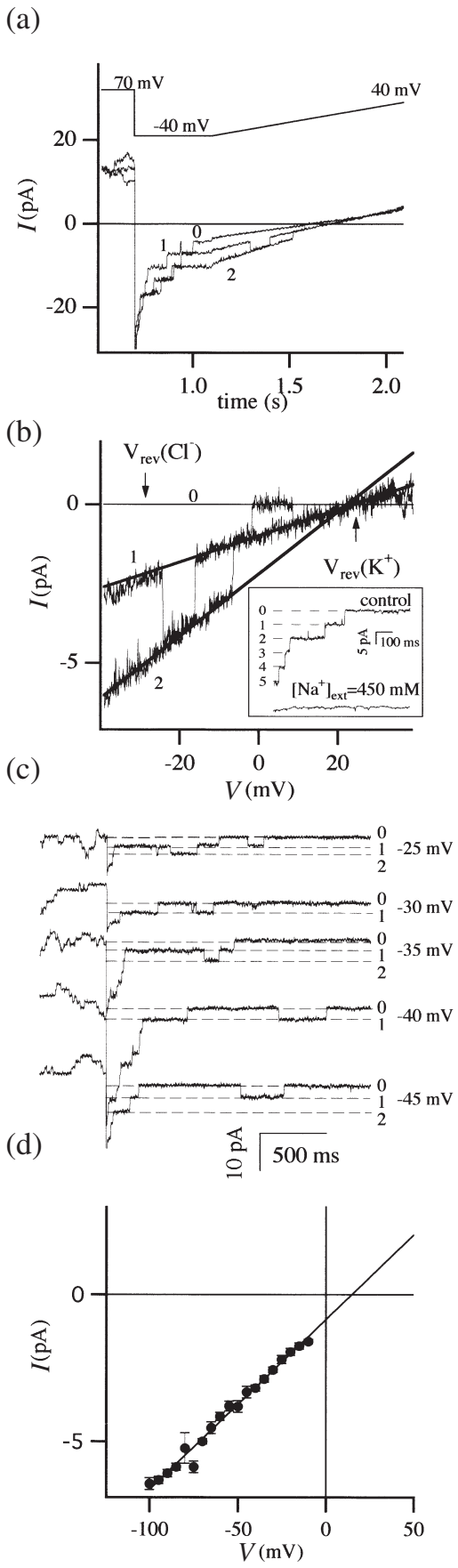

Figure 7. Outward single channel recordings in *Posidonia oceanica* protoplasts. (a) Single channels were recorded by applying the voltage protocol shown at the top of the figure. Numbers 0, 1 and 2 indicate that 0, 1 or 2 channels are open in the current records shown below. (b) The same currents displayed in (a) (during the application of the voltage ramp) after the subtraction of the leakage. The continuous lines represent the linear fitting of data and gave an open channel conductance of 58 pS. 0, 1 and 2 have the same meaning as in (a). The arrows show the reversal potentials for Cl^- (V_{nernst} = –29 mV) and K^+ (V_{nernst} = +25 mV), calculated using the Nernst equation. Inset: single outward channel recordings elicited in the same patch by tail potentials to –90 mV after a prepulse to +100 mV in the presence of 450 mM KCl in the bath solution (upper trace, control) and in 450 mM NaCl (lower trace). (c) A series of single channel recordings, activated by a prepulse potential to –10 mV (first segment), can be observed at negative tail potentials of increasing amplitude (from –25 to –45 mV). Numbers 0, 1, 2 have the same meaning as in (a). (d) Single channel amplitudes derived from traces like those shown in (c) plotted as a function of tail potentials. In accordance with the data obtained from continuous voltage ramps (b), the best fits gave a single channel conductance of 58 ± 2 pS. Standard ionic solutions.

to both sodium and potassium ions (Fig. 10c & d) as well as to anions (the reversal potential is almost 0 mV in asymmetric ionic solutions (Fig. 10c & d); and (5) marked and reversible inhibition when TEA^+ and lanthanum (Fig. 10e) were added to the external bath solution.

Lanthanum, which was occasionally used to improve the quality of the seal (Carpaneto *et al*. 2003) or to inhibit the non-selective currents, slowed the activation and de-activation kinetics of the outward currents only slightly. Extraplasmatic lanthanum (1 mM) only determined a moderate shift (approximately 10 mV towards more positive potentials) of the Boltzmann characteristics and a slight (5%) decrease in the outward currents at saturating voltages and a 10% decrease in the instantaneous tail currents of the outward currents at large hyperpolarizing membrane potentials (not shown).

DISCUSSION

The nature of the cells used in our electrophysiological characterization can be inferred from a comparison of the dimensions from one side of the patched protoplasts, on the other of the cells (parenchyma, epidermis and sheath) identified and measured in micrographs of *P. oceanica* leaves (Figs 1 and 2). We focused our attention on an apparently homogeneous population of protoplasts with an intermediate size in the order of 13 μm; we systematically patched these protoplasts, disregarding those that were either too small or too large (occasionally present in the preparation). The mean size of the patched protoplasts is very close to the equivalent radius (derived from digital imaging measurements) of sheath cells (10.6 μm) surrounding the vascular bundles. In comparison, from digital imaging measurements, parenchyma and epidermis cells displayed a mean radius of 19.4 and 7.8 μm, respectively. It should be noted that in seagrasses the longitudinal veins of the leaves

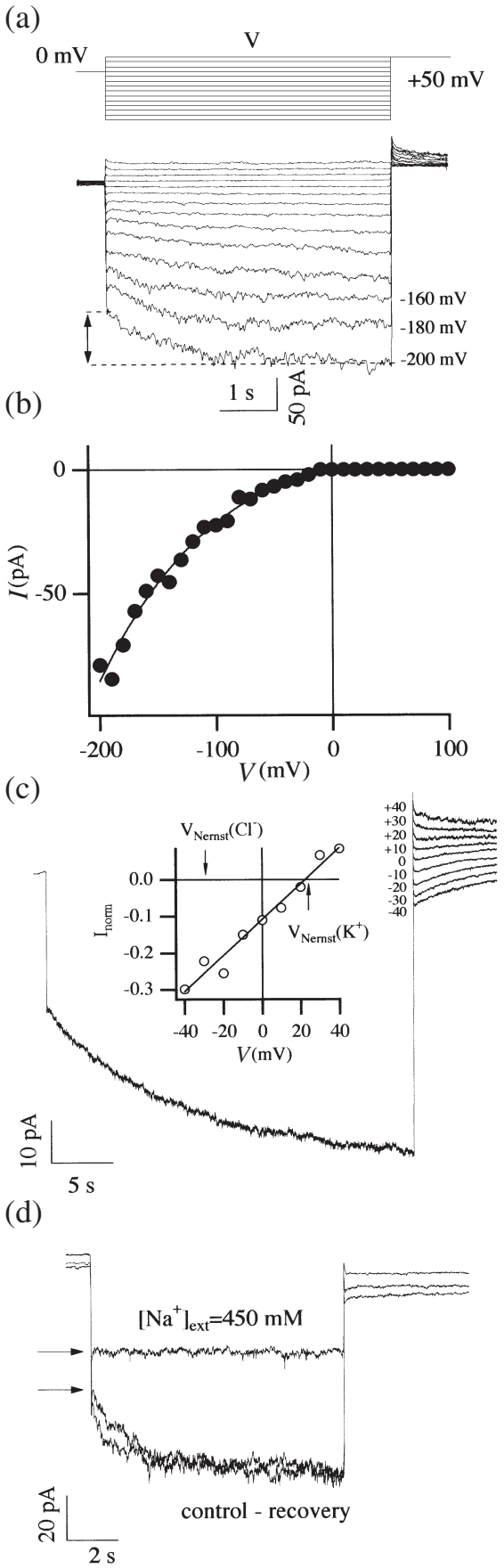

Figure 8. Macroscopic inward-rectifying currents in protoplasts from *Posidonia oceanica* leaves. (a) Inward currents elicited by a series of voltage pulses ranging from +80 mV to –200 mV in –20 mV decrements. Holding and tail membrane potentials: 0 mV and +50 mV, respectively. The upper trace illustrates the applied voltage protocol. (b) Current-voltage characteristics of the records shown in (a) (note that only one over two current records is reported in (a), for clarity). The current data are corrected for the leakage by subtracting the initial value of the current from the steady-state value for each current record. (c) Tail currents elicited by membrane potentials ranging from –40 to +40 mV in 10 mV increments. The channels were activated by a hyperpolarizing pulse to –200 mV for 30 s. Inset: Normalized tail currents (I_{norm}) versus applied voltage. I_{norm} was obtained as follows: (i) tail currents were fitted with the exponential function $I_t = A_0 + A_1\exp(-(t - t_0)/\tau)$; (ii) the steady-state current at –200 mV (I_s) was calculated from $I_s = I_{final} - I_{initial}$; (iii) I_{norm} was obtained from the equation $I_{norm} = A_1/I_s$. The arrows show the reversal voltage of Cl^- ($V_{nernst} = -29$ mV) and K^+ ($V_{nernst} = +25$ mV), calculated using the Nernst equation. (d) Illustrates Na^+ permeability through the inward channel. Currents elicited by a voltage pulse to –200 mV in asymmetric standard solutions (control and recovery, $[K^+] = 450$ mM) and after that potassium of the external solution had completely been replaced by an equimolar concentration of sodium ($[Na^+] = 450$ mM). Holding and tail voltages were –50 mV and –100 mV, respectively.

are enclosed by a distinct layer of sheath cells which is lignified in mature leaf blades (Kuo & McComb 1989) whereas in the youngest leaves the thickening of the sheath cell wall is at the very beginning. Moreover, the average number of sheath cells surrounding the vascular bundles, which are exposed to the enzymatic digestion at the leaf cross section (see Fig. 1b & c), is presumably smaller but of the same order of magnitude as the number of epidermis cells. On the basis of previous considerations, although we cannot exclude that some patched protoplasts may have been from parenchyma or epidermal cells, this remains a rather improbable event.

In *Posidonia* protoplasts, we recorded ion currents which were ascribed to the activation of an outward-rectifying time-dependent channel selective for potassium ions. This channel was impermeable to sodium and to other monovalent cations and displayed functional characteristics resembling those of GORK and SKOR, the outward-rectifying channels identified in *A. thaliana* guard cells and xylem parenchyma cells (Gaymard *et al*. 1998; Ache *et al*. 2000; Lacombe *et al*. 2000). This family also comprises SPORK (from *Samanea saman* (Moshelion *et al*. 2002) and PTORK [from *Populus tremula* (Langer *et al*. 2002)].

As in GORK/SKOR channels, but unlike the outward potassium channel identified in the halophytic angiosperm *Zostera muelleri* (Garrill *et al*. 1994), the voltage sensitivity of the *Posidonia* outward channel depends on the concentration of external potassium, as the current-voltage characteristics shifted (by –63 mV) towards negative potentials when the external potassium concentration was decreased (by 440 mM). A similar behaviour of the gating mechanisms, where the g–V curve of outward potassium channels shifts to the right along the voltage-axis with the K^+ reversal

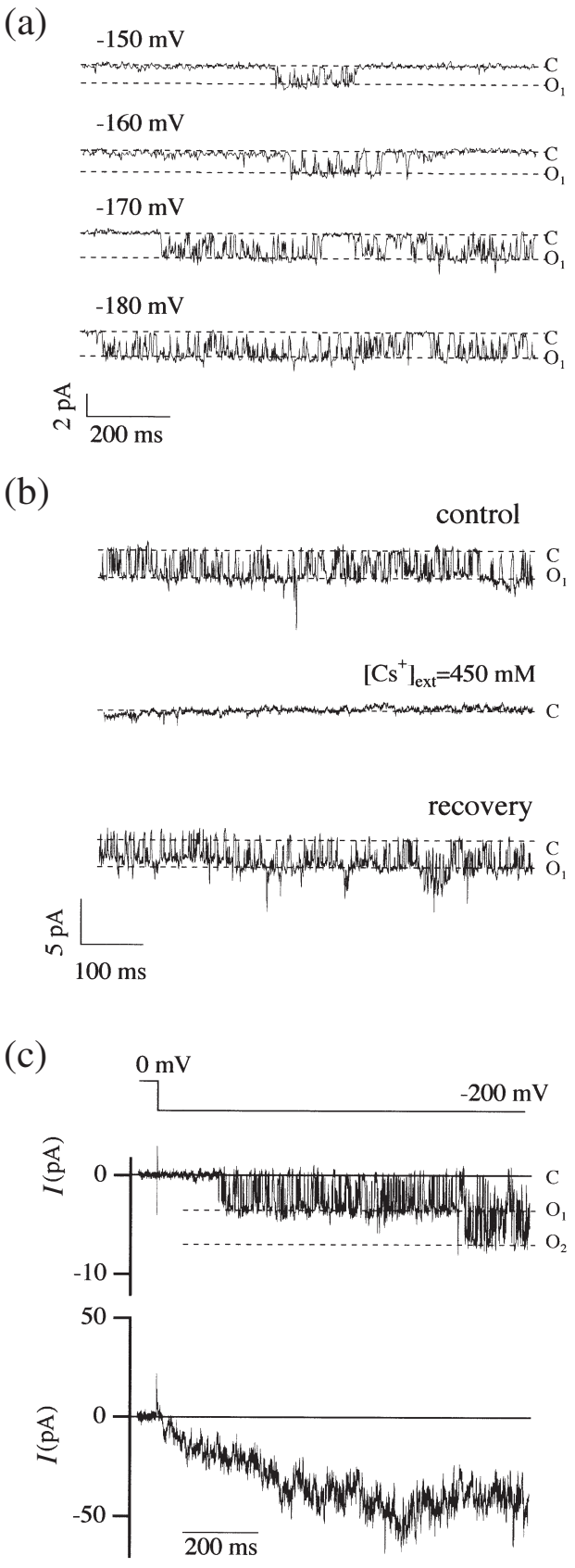

Figure 9. Inward single channels in excised patches from *Posidonia oceanica* protoplasts. (a) Recordings displaying an increasing open probability of an inward-rectifying single channel elicited by hyperpolarizing membrane potentials of increasing amplitude in outside-out excised patches. (b) External Cs^+ does not permeate through inward single channels. Applied membrane potential –200 mV. (c) A single channel trace recorded applying a step pulse to –200 mV and (lower trace) reconstruction of a macroscopic current obtained by averaging 19 single traces.

potential, has been described in guard cells of terrestrial plants (Blatt 1991; Blatt & Gradman 1997). This shift was ascribed to the binding of potassium ions acting in a co-operative manner at the external surface of the membrane, deep within the membrane electrical field, but in a site distinct from the channel pore. It has been suggested that potassium affects the channel-gating binding to a site which has a structure similar to that of the channel pore. Actually, the shift of g–V (inhibition at large K^+ concentrations) is observed also in the presence of other cations that are efficient substitutes of potassium. The efficiency in shifting the g–V increases in parallel with the selectivity properties of the channel for the cation examined (Blatt & Gradman 1997). In *P. oceanica*, the shifts of the g–V characteristics and the different kinetics of current activation induced by different cations (such as Cs^+, Li^+ and Na^+ as described in Fig. 6) are in accordance with this allosteric model; specifically the conductance shift in the *P. oceanica* outward channel is smaller in the presence of Cs^+, which has a better accessibility to the pore with respect to Li^+ and Na^+. This indicating that, contrary to Li^+ and Na^+, caesium is an effective substitute for extracellular K^+ in the binding site, whereas substitution by Na^+ and Li^+ has consequences equivalent to low potassium concentration.

Therefore, as for the guard cell outward potassium channel, the gating of the *Posidonia* outward channel seems to be also able to accommodate significant changes in the electrochemical driving force; this mechanism possibly guarantees that K^+ movement is directed out of the cell regardless of the conditions of the external solution (Blatt & Gradman 1997). Working under the hypothesis that protoplasts derive from sheath vascular bundles, the outward-rectifying channel could play in *P. oceanica* a role similar to that hypothesized for SKOR in *Arabidopsis thaliana* root stelar tissues; namely, in *Posidonia* it could be involved in potassium release from the sheath cells to xylem vessels.

The time course of activation of a *Posidonia* outward channel is between 50 and 100 ms and does not depend significantly on the applied membrane potential. Interestingly, the activation kinetics of the outward currents in *Posidonia* are comparable with those of GORK and SKOR (Gaymard *et al*. 1998; Ache *et al*. 2000) but much faster than the kinetics measured in *Z. muelleri*, whose outward currents include two components, with the slowest component in the order of a few seconds (Garrill *et al*. 1994). It should be observed that experiments on *Z. muelleri* were performed in external solutions with a much lower ionic strength than that used in our experiments.

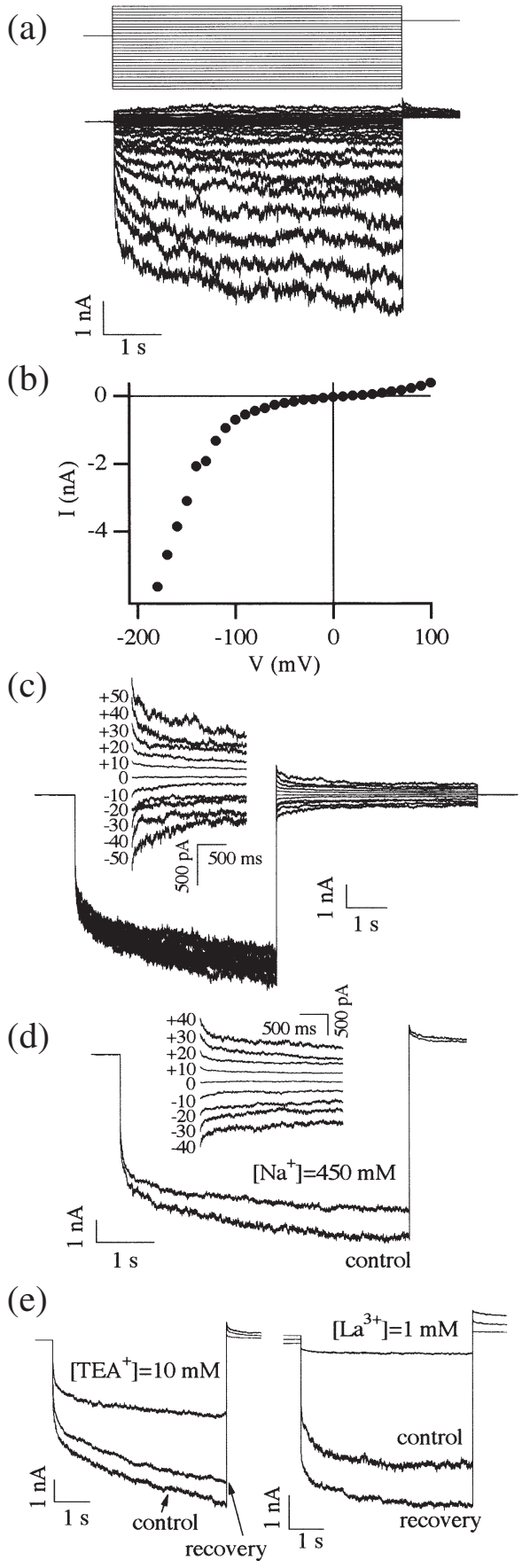

Figure 10. Non-selective channels in *Posidonia oceanica* protoplasts. (a) Family of time-dependent currents mediated by non-selective channels occasionally recorded in *P. oceanica* protoplasts. (b) Current-voltage characteristics of the data shown in (a). Holding and tail potentials equal to 0 mV and +50 mV, respectively. (c) In standard ionic solutions, after a step pulse to –180 mV, tail currents display a reversal voltage at approximately 0 mV. (d) Tail currents obtained when the external potassium was substituted by an equimolar concentration of sodium. Panels (c) and (d) suggest that these inward currents are mediated by non-selective ion channels. (e) The non-selective time-dependent currents are partially and reversibly inhibited by 10 mM TEA^+ and almost completely and reversibly inhibited by 1 mM La^{3+}. Holding, step and tail potentials were +10 mV, –200 mV and +50 mV in (d) and 0 mV, –150 mV and +50 mV in (e), respectively.

Notably, in comparison with outward potassium channel in *Z. muelleri* (which was only five times more permeable to potassium than sodium) the *P. oceanica* outward channel displayed a marked selectivity for K^+ over Na^+ and other monovalent alkaline cations. This is demonstrated by the agreement of the reversal potential with the K^+ Nernst potential and by the total absence of tail currents when K^+ was substituted by equimolar concentrations of Na^+ or Li^+ or Cs^+. This confirms that, in this channel, sodium permeability is definitely very low in comparison with potassium.

The single channel conductance of the *Posidonia* outward potassium channel (58 pS) is comparable with the conductance of the outward potassium channels in *Z. muelleri* (70 pS), despite the much lower ionic activity of the solution used in *Z. muelleri* experiments. However, one should take into account that the *Posidonia* channel might be subjected to a saturation of the conductance at large K^+ concentration (Gambale *et al*. 1996).

We also recorded a small inward time-dependent current which activated at hyperpolarizing membrane potentials more negative than –50 mV. As in *Z. muelleri*, in *P. oceanica* this time-dependent current was always associated with a time- and voltage-independent component characterized by an almost linear behaviour all over the voltage range (positive and negative) investigated. As the outward channel, the time-dependent component of the inward channel also showed selectivity for potassium and was almost impermeable to Na^+ on the contrary, the time-independent component was not selective and could even represent a membrane leakage.

The highly selective *P. oceanica* time-dependent inward channel should be compared with the homologous channel measured in *Z. muelleri*, which instead is at least partially permeable to Na^+ (Garrill *et al*. 1994).

Interestingly, the time-dependent inward potassium currents activate at potentials (–50 mV) which are comparable with the potentials eliciting inward currents in protoplasts from *Z. muelleri* leaves (Garrill *et al*. 1994); on the contrary, similar inward potassium channels from terrestrial plants display thresholds of activation which typically are more negative than approximately –80 mV (Müller-Röber *et al*. 1995; Hedrich & Dietrich 1996; Reintanz *et al*. 2002) or

even approximately –120 mV (Bregante, Gambale & Lo Schiavo 1996; Amtmann 1999).

A third type of current was occasionally recorded at hyperpolarizing membrane potentials. This current displayed time- and voltage-dependent components mediated by non-selective ion channels. The contribution of this channel to the currents could be easily identified as it was partially and reversibly inhibited by the addition of 10 mM TEA^+ to the bath solution and almost completely and reversibly blocked by La^{3+} (Fig. 10). One could speculate that this channel might be responsible for sodium or anion movements in *Posidonia* leaf cells.

In addition to providing information for the identification of the permeation pathways of nutrients and toxic ions in seagrasses, these studies may be useful for future cloning of a *P. oceanica* channel.

ACKNOWLEDGMENTS

The technical assistance provided by G. Gaggero, G. Boido and D. Magliozzi was greatly appreciated.

REFERENCES

Ache P., Becker D., Ivashikina N., Dietrich P., Roelfsema R.G. & Hedrich R. (2000) GORK, a delayed outward rectifier expressed in guard cells of *Arabidopsis thaliana*, is a K^+-selective, K^+-sensing ion channel. *FEBS Letters* **486,** 93–98.

Amtmann (1999) K^+selective inward-rectifying channels and apoplastic pH in barley roots. *Plant Physiology* **119,** 331–338.

Amtmann A. & Sanders D. (1999) Mechanisms of Na^+ uptake by plant cells. *Advances in Botanical Research* **29,** 75–112.

Arai M., Pak J.Y., Nomura K. & Nitta T. (1991) Seawater-resistant, non-spherical protoplasts from seagrass leaves. *Physiologia Plantarum* **83,** 551–559.

Balestri E. & Cinelli F. (1992) Isolation of protoplasts from the seagrass *Posidonia oceanica* (L.) Delile. *Aquatic Botany* **43,** 301–304.

Balestri E. & Cinelli F. (2001) Isolation and cell wall regeneration of protoplasts from *Posidonia oceanica* and *Cymodocea nodosa* *Aquatic Botany* **70,** 237–242.

Blatt M.R. (1991) Ion channel gating in plants: physiological implications and integration for stomatal function. *Journal of Membrane Biology* **124,** 95–112.

Blatt M.R. & Gradmann D. (1997) K^+-Sensitive gating of the K+ outward rectifier in *Vicia* guard cells. *Journal of Membrane Biology* **158,** 241–256.

Blumwald E., Aharon G.S. & Apse M.P. (2000) Sodium transport in plant cells. *Biochemica et Biophysica Acta* **1465,** 140–151.

Bregante M., Gambale F. & LoSchiavo F. (1996) Ionic transport in the plasma membrane of carrot protoplasts from embryogenic cell-suspension cultures. *FEBS Letters* **380,** 97–102.

Brinn N.T. & Pickett J.P. (1979) Glycol methacrylate for routine, special stains, histochemistry, enzyme histochemistry and immunohistochemistry. *Journal of Histochemistry* **2,** 125–130.

Buchanan B.B., Gruissem W. & Jones R.L. (2000) *Biochemistry and Molecular Biology of Plants.* American Society of Plant Physiologists, Waldorf, MD, USA.

Carpaneto A., Cantù A.M., Busch H. & Gambale F. (1997) Ion channels in the vacuoles of the seagrass *Posidonia oceanica*. *FEBS Letters* **412,** 236–240.

Carpaneto A., Cantù A.M. & Gambale F. (1999) Redox agents regulate ion channel activity in vacuoles from higher plant cells. *FEBS Letters* **442,** 129–132.

Carpaneto A., Magrassi R., Zocchi E., Cerrano C. & Usai C. (2003) Patch-clamp recordings in isolated sponge cells (*Axinella polypoides*). *Journal of Biochemistry and Biophysics Methods* **55,** 179–189.

Feder N. & O'Brien T.P. (1968) Plant microtechnique: some principles and new methods. *American Journal of Botany* **55,** 123–142.

Gambale F., Bregante Stragapede M., : F. & Cantù A.M. (1996) Ionic channels of the sugar beet tonoplast are regulated by a multi-ion single-file permeation mechanism. *Journal of Membrane Biology*. **154,** 69–79.

Garrill A., Tyerman S.D. & Findlay G.P. (1994) Ion channels in the plasma membrane of protoplats from the halophytic angiosperm *Zostera muelleri*. *Journal of Membrane Biology* **142,** 381–393.

Gaymard F., Pilot G., Lacombe B., Bouchez D., Bruneau D., Boucherez J., Michaux-Ferriere N., Thibaud J.B. & Sentenac H. (1998) Identification and disruption of a plant shaker-like outward channel involved in K^+ release into the xylem sap. *Cell* **94,** 647–655.

Hedrich R. & Dietrich P. (1996) Plant K^+ channels: similarity and diversity. *Botanica Acta* **109,** 1–8.

Ivashikina N., Becker D., Ache P., Meyerhoff O., Felle H.H. & Hedrich R. (2001) K+ channel profile and electrical properties of *Arabidopsis* root hairs. *FEBS Letters* **508,** 463–469.

Kuo J. & McComb A.J. (1989) Seagrass taxonomy, structure and development. In *Biology of Seagrasses* (eds A.W.D. Larkum, A.J. McComb & S.A. Shepherd), pp. 6–73. Elsevier. Science Publishers, Amsterdam, The Netherlands.

Lacombe B., Pilot G., Gaymard F., Sentenac H. & Thibaud J.B. (2000) pH control of the plant outwardly-rectifying potassium channel SKOR. *FEBS Letters* **466,** 351–354.

Langer C., Ache P., Geiger D., Stinzing A., Arend M., Wind Regan S., Fromm J. & Hedrich R. (2002) Poplar potassium transporters capable of controlling K^+ homeostasis and K^+-dependent xylogenesis. *Plant Journal* **32,** 997–1009.

Mariani Colombo P., Rascio N.C. & Cinelli F. (1983) Posidonia oceanica (L.) DELILE: a structural study of the photosynthetic apparatus. *Marine Ecology* **4,** 133–145.

Moshelion M., Becker D., Czempinski K., Mueller-Rober B., Attali B., Hedrich R. & Moran N. (2002) Diurnal and circadian regulation of putative potassium channels in a leaf moving organ. *Plant Physiology* **128,** 634–642.

Müller-Röber B., Ellenberg J., Provart N., Willmitzer L., Busch H., Becker D., Dietrich P., Hoth S. & Hedrich R. (1995) Cloning and electrophysiological analysis of KST1, an inward rectifying K^+ channel expressed in potato guard cells. *EMBO Journal* **14,** 2409–2416.

Procaccini G. & Mazzella L. (1996) Seagrass biology. In *Proceedings of an International Workshop* (eds J. Kuo, R.C. Phillipps, D.I. Walker & H. Kirkman). pp. 85–92. Rottnest Island, Western Australia.

Procaccini G. & Mazzella L. (1998) Population genetic structure and gene flow in the seagrass *Posidonia oceanica* assessed using microsatellite analysis. *Marine Ecology Progress Series* **169,** 133–141.

Reintanz, Szyroki A., Ivashikina N., Ache P., Godde M., Becker D., Palme K. & Hedrich R. (2002) AtKC1, a silent *Arabidopsis* potassium channel a-subunit modulates root hair K^+ influx. *Proceedings of the National Academy of Sciences of the USA* **99,** 4079–4084.

Tyerman S.D. (1989) Solute and water relations of seagrass. In *Biology of Seagrasses* (eds A.W.D. Larkum, A.J. McComb &

S.A. Shepherd), pp. 723–759. Elsevier. Science Publishers, Amsterdam, The Netherlands.

White P.J. (1999) The molecular mechanism of sodium influx to root cells. *Trends in Plant Science* **4,** 245–246.

Wood M.J. & Korn S.J. (2000) Two mechanisms of K^+-dependent potentiation in Kv2.1 potassium channels. *Biophysics Journal* **79,** 2535–2546.

Received 11 August 2003; received in revised form 6 October 2003; accepted for publication 7 October 2003